Early Classification of Motor Tasks Using Dynamic Functional Connectivity Graphs from EEG

Foroogh Shamsi, Ali Haddad, and Laleh Najafizadeh

Integrated Systems and NeuroImaging Laboratory, Department of Electrical and Computer Engineering, Rutgers University, Piscataway, NJ, 08854 USA

E-mail: {foroogh.shamsi,ali.haddad,laleh.najafizadeh}@rutgers.edu

July 2020

Abstract. *Objective.* Classification of electroencephalography (EEG) signals with high accuracy using short recording intervals has been a challenging problem in developing brain computer interfaces (BCIs). This paper presents a novel feature extraction method for EEG recordings to tackle this problem. *Approach.* The proposed approach is based on the concept that the brain functions in a dynamic manner, and utilizes dynamic functional connectivity graphs. The EEG data is first segmented into intervals during which functional networks sustain their connectivity. Functional connectivity networks for each identified segment are then localized, and graphs are constructed, which will be used as features. To take advantage of the dynamic nature of the generated graphs, a Long Short Term Memory (LSTM) classifier is employed for classification. *Main results.* Features extracted from various durations of post-stimulus EEG data associated with motor execution and imagery tasks are used to test the performance of the classifier. Results show an average accuracy of 85.32% using features extracted from only 500 ms of the post-stimulus data. *Significance.* Our results demonstrate, for the first time, that using the proposed feature extraction method, it is possible to classify motor tasks from EEG recordings using only few hundreds of milliseconds of the data. This duration is considerably shorter than what has been reported before. These results will have significant implications for improving the effectiveness and the speed of BCIs, particularly for those used in assistive technologies.

Keywords: Electroencephalography (EEG), Brain Dynamics, Dynamic Functional Connectivity, Dynamic Graphs, Brain Computer Interface (BCI), Long Short Term Memory (LSTM).

1. Introduction

Brain computer interfaces (BCIs) are designed to establish a communication link between the human brain and external devices. BCIs offer the possibility of generating commands from brain recordings to control external devices such as those used in assistive technologies. Among different types of BCIs, electroencephalography (EEG)-based BCIs have received considerable attention in the BCI research community due to their advantages including non-invasiveness, high temporal resolution, low-cost, and portability [1, 2].

Two important metrics that impact the performance of BCIs and influence their efficiency and practicality in different applications are 1) the buffering lag, *i.e.* the duration of recordings required by the classification algorithm to create commands (which largely determines the speed of the BCI), and 2) the classification accuracy (which determines the reliability of the BCI). Clearly, an algorithm capable of classifying a number of different tasks with high accuracy using a "short" interval of recordings is of great interest.

In EEG-based BCIs, motor imagery (MI) tasks, targeting imagination of different forms of muscle movements, such as arms, hands, tongue, and legs, are popular and have been commonly used. To this date, numerous classification algorithms, utilizing various feature extraction and classification techniques have been used in EEG-based BCIs for decoding motor execution/imagery tasks [3]. To provide an overview of recent work in this domain, in Table 1‡, a comparison of recent work is given. These studies have been categorized into different groups based on the buffering lag, which is the duration of the data that needs to be collected before a prediction can take place. Based on their buffering lag, we divided the existing studies into three groups of $1-2$ s, $2-4$ s, and equal or greater than 4 s. For each study, we have summarized information on the number of classes, number of EEG electrodes (channels), feature extraction domain (time, frequency, time-frequency), classification algorithm, and reported classification accuracy.

From Table 1, one can see that the majority of studies have considered two-class problems. The highest accuracy results for two-class problems were reported in [4] for using $1-2$ s of data, in [5, 6, 7, 8, 9] for using $2-4$ s of data, and in [10] for using equal or greater than 4 s of data. For multi-class problems, the highest accuracy results were achieved in [11] for using $1-2$ s of data, in [9, 12, 13] for using $2-4$ s of data, and in [14, 15, 16] for using equal or greater than 4 s of data. Considering these studies, it can be concluded that with respect to the required buffering lag, the decoding process has been relatively slow. This slowness causes challenges in BCI applications, where a sequence of commands needs to be decoded and executed in order to complete a task, such as moving a robotic arm from one place to another. There is therefore, a crucial need to develop new methods capable of early decoding of EEG signals to improve

‡ Note that due to high volume of papers in this field, we only considered highly-cited studies that considered classification of motor-related tasks, and were published after 2014.

the efficiency of BCIs. In this paper, we aim to target this problem, and propose a framework, which requires a duration of only a few hundreds of milliseconds of EEG data to achieve high accuracy in classification.

Our proposed approach is based on functional connectivity and the hypothesis that for the execution of tasks, the brain relies on dynamic interactions among its different regions [17, 18, 19, 20]. Previous work [21, 22, 23, 24] have indicated that brain's functional connectivity throughout the course of movement-related (execution/imagery) tasks can be used to study the underlying mechanisms involved in performing those tasks. These results suggest the potential of acquiring useful information from functional connectivity networks for discriminating various motor-related tasks, which can also be used in BCIs. Indeed, functional connectivity has been utilized in recent EEG-based BCI work. As an example, in [25], phase-locking value (PLV) was used to estimate functional connectivity patterns from EEG recordings. The authors then identified node-pairs in constructed functional networks that discriminate resting state vs motor imagery tasks. Using this information along with a subject-specific frequency band selection procedure, features were extracted to discriminate left and right hand motor imagery tasks, where an average classification accuracy of 64.27% was achieved. In another connectivity-BCI study [26], after identifying functional connectivity patterns using partial directed coherence metric, a statistical selection method based on the appearance rate of directed connectivities and larger partial directed coherence magnitude was used to characterize task-specific functional connectivity networks. The identified networks were then used as features and an average classification accuracy of 78.76% for discriminating right hand vs right foot motor imagery tasks was reported. In [27], the feasibility of using functional connectivity patterns for classification of motor imagery (left vs right hand) was explored. In this study, interactions among EEG electrodes were modeled as graphs which were constructed using motif synchronization method, and then, various graph metrics were used as features for the classification problem. The results of this study demonstrate the feasibility of using graph methods for the classification of motor imagery tasks. In another work [23], a recurrence-based method for brain functional connectivity network estimation was proposed, and graph measures were computed and employed as features for decoding motor imagery tasks, resulting in an average classification accuracy of 71.5% for different pairs of left hand, right hand, foot, and tongue motor imagery tasks. In [11], connectivity graph measures combined with channel-based time/frequency domain features were employed for classifications of motor imagery tasks, and an average accuracy of 79.69% was reported for a 4-class motor imagery classification. These studies demonstrate the feasibility of using functional connectivity networks for decoding motor-movement tasks in BCIs. However, as seen in Table 1, in these functional connectivity-based BCI studies, features were extracted from durations of equal or greater than 2 s. As for dynamics, dynamic brain functional networks corresponding to motor imagery tasks during the event-related synchronization (ERS) and de-synchronization (ERD) periods were investigated in [22], where it was shown that different stages of motor preparation and imagery

can be characterized by network measures. Their findings demonstrated that the underlying dynamic information processing during motor imagery tasks can be described by dynamic functional connectivity networks, suggesting the potential for using dynamic functional connectivity in BCIs. In [28], empirical mode decomposition phase locking method was used to model the functional connectivity between EEG channels, and time-frequency connectivity maps were generated by computing time-dependent mean clustering coefficients of graph nodes for different frequency bands. A Hidden Markov Model (HMM) was then employed to classify the dynamics of the mean clustering coefficients in different frequency bands, indicating that the dynamics of functional connectivity networks could provide useful information for differentiating motor tasks.

Table 1: Performance comparison of recent studies for classification of MI tasks in EEG-based BCIs.

Time (s)	**Year**	# of **Classes**	# of **Channels**	**Feature Domain**	**Classifier**	**Average Accuracy(%)**	**Ref.**
$1-2$	2016	2	3	Time & Frequency	GA-PSO Based k-means Clustering	60.97	[29]
	2018	2	15	Time	RF	72.73	[30]
	2014	2	128	Frequency	SVM	77.11	[31]
	2014	2	4	Time & Frequency	LDA	77.3	[32]
	2017	2	118/3	Time	NBPW	76.12/86.41	[33]
	2019	2/2	2/2	Frequency	SVM	78.04/83.58	[4]
	2019	4	22	Time	Multi-branch 3D CNN	75.02	[34]
	2019	4	22	Time & Frequency	SRDA	79.7	[11]
$2-4$	2016	2	22	Time & Frequency	SVM	64.27	[25]
	2016	2	118	Time	DNN with LRP	71.6	[35]
	2014	2	27	Time	NBPW	74.14	[36]
	2016	2	22	Time & Frequency	SVM	74.92	[37]
	2018	2	22	Time	LSTM	75.28	[38]
	2019	2	3	Frequency	Capsule Network	78.44	[39]
	2017	2	118	Frequency	Mahalanobis Distance	78.76	[26]
	2014	2	22/32	Time	Minimum Distance	78/80	[40]
	2019	2	15	Time & Frequency	LDA/SVM	79.19	[41]
	2018	2	22	Time & Frequency	MDRM	79.93	[42]
	2016	2	14	Time	RF	80.05	[43]
	2017	2	3	Time	SBL	81.7	[44]
	2016	2	59/118	Time	SVM	78/83.3	[45]
	2017	2	3/2/40	Frequency	BTSPRT	83.4	[46]
	2018	2	59	Time	SVM	84.86	[47]
	2019	2	3	Time & Frequency	SVM	85	[48]
	2015	2	118/60 /22	Time	FLDA	84.04/83.77 /85.52	[49]
	2016	2	60/118	Time & Frequency	DPL	85.7/80.77	[50]
	2018	2	18	Time	Ensemble Classification	86.23	[51]
	2018	2	60/22 /3	Time & Frequency	SVM	88.5/83.25 /84.3	[52]
	2015	2	118	Frequency	-	90.7	[53]
	2016	2	32	Time	SVM	90.9	[54]
	2019	2	118/60 /22	Time	MDRM	87.21/90.93 /80.98	[55]
	2018	2	64	Time	ELM	91	[56]
	2019	2	3	Time & Frequency	HS-CNN	91.57/87.6	[57]
	2017	2	18/59 /3	Time	LDA/SVM	91.68/82.34 /81.02	[58]
	2015	2	118	Time	SVM	81/92	[59]

Continue on the next page

Table 1: Continued from previous page

Time (sec)	**Year**	**# of Classes**	**# of Channels**	**Feature Domain**	**Classifier**	**Average Accuracy(%)**	**Ref.**
	2015	2	14/118	Time	SVM	80.88/92.29	[60]
	2017	2	118	Time & Frequency	kNN	92.8	[61]
	2014	2	118	Time	LR	93.91	[62]
	2017	2	2	Time	Hierarchical ELM	94.54	[5]
	2016	2	118	Time	NB	96.36/91.97	[6]
	2018	2	118	Time	SVM	96.89	[7]
	2018	2	10	Time & Frequency	SVM	97.56	[8]
	2015	2/3	32	Time & Frequency	LDA/LR/SVM	66.9/60.7	[63]
	2015	3	118	Time	-	68.94	[64]
	2016	3	64	Time	Multi-Class Adaboost	79.5	[65]
	2020	3	27	Time & Frequency	SVM/ELM	99.38	[66]
	2019	2/4	22	Time	LS	71.5/49	[23]
	2016	4	22	Frequency	RF	68.32	[67]
	2018	2/3/4	64	Time	CNN	83.49/79.25/68.51	[68]
	2018	4	22	Time	Multi-Class Multi-Kernel RVM	70.3	[69]
	2015	2/4	118/60	Time & Frequency	SVM	69.40/71.22	[70]
	2019	4	22	Time	CNN	74	[71]
	2018	4	22	Time & Frequency	SVM	75.47	[72]
	2015	2/2/4	59/62/62	Frequency	Hierarchical SVM	85.2/94.1/83.2	[9]
	2015	7	32	Frequency	Bayesian	62.9	[12]
	(2019)	4/5	22/8	Time & Frequency	CNN	80.03/76.62	[13]
≥ 4	2014	2	64	Time	SVM	78	[73]
	2019	2	59	Time	Regularized LDA	77	[74]
	2019	2	3	Time	SVM/Ensemble learning learning	80	[75]
	2019	2	3	Time & Frequency	SVM	80.7	[76]
	2014	2	3/2	Time & Frequency	BPNN & SVM	80.8	[77]
	2018	2	22	Time	Information Fusion	81.87	[78]
	2014	2	2	Time & Frequency	AFNN	82.5	[79]
	2016	2	3	Frequency	RBM	84	[80]
	2017	2	3/118/118	Time	LDA	81.23/84.08/73.71	[81]
	2019	2	64/118/3	Time & Frequency	GSLDA	84.8	[82]
	2017	2	9	Time	Fuzzy SVM	86.25	[83]
	2017	2	118	Time & Frequency	WNB	86.38	[84]
	2018	2	118/3	Time	Multi-Kernel ELM	87.5/78.9	[85]
	2018	2	3	Time & Frequency	SVM	88.36	[86]
	2015	2	6/7	Time	IT2FLS	90.10/56.67	[87]
	2016	2	59	Time	PSO-SVM	90.20/85.25	[88]
	2015	2	2	Time & Frequency	LDA	90.71	[89]
	2015	2	64/3	Time & Frequency	SVM	92.86/72.3	[90]
	2019	2	32	Time & Frequency	LSTM/pCNN /RCNN	84.24/92.28/77.72	[91]
	2018	2	64	Time	LDA/SVM	99	[27]
	2016	3	15	Time	LDA	63	[92]
	2014	3	22	Time	SVM	86.25	[93]

Continue on the next page

Table 1: Continued from previous page

Time (sec)	**Year**	# of **Classes**	# of **Channels**	**Feature Domain**	**Classifier**	**Average Accuracy(%)**	**Ref.**
	2016	3/4	32/22	Frequency	NBPW and	59.23/38.07	[94]
	2019	2/3/4	64	Time & Frequency	LSVM/KSVM/ GB/SRDA	93.6/71.9 /58.3	[95]
	2017	4	22	Time	Hierarchical SVM	64.4/69.16	[96]
	2014	4	18	Time	Decision Tree	65.35	[97]
	2016	4	64	Frequency	SVM	65/74.14	[98]
	2015	2/4	64/3	Time	Twin SVM	100/74.5	[10]
	2014	4	60	Time & Frequency	SVM	76.87	[99]
	2015	4	22	Time	SUSS-SRKDA	77	[100]
	2016	4	17	Time & Frequency	Mahalanobis Distance	81.4	[14]
	2017	4	2	Time	RANFN	85.5	[15]
	2019	4	22/128	Time	CPMS-CNN	74.3/94.7	[16]

Motivated by the results of functional connectivity-based BCIs, in this paper, we propose a new framework that utilizes the spatial and temporal (dynamic) characteristics of brain functional networks for early decoding of motor execution and imagery tasks. Our hypothesis is that for different movement execution/imagery tasks, the "*spatial*" distribution of the brain functional networks as well as their "*dynamics*" provide discriminatory information for the classification problem, even within a short interval after the task onset.

In the proposed framework, EEG recordings are first segmented using our recently proposed segmentation method to identify the time intervals (segments) during which the spatial distribution of the underlying functional networks stays quasi-stationary [101, 102, 103]. Functional connectivity networks for each identified segment are then localized to generate functional connectivity graphs. The resulting graphs, extracted from the sequences of the segments, are then vectorized and passed to the classifier. Considering the dynamic nature of the extracted functional connectivity graphs, we employ a long short-term memory (LSTM) network as the classifier, which allows for using the information in sequence. To evaluate the early decoding capability of the proposed framework, we use the sequence of functional connectivity graphs extracted from interval with different post-stimulus durations starting at few hundreds of milliseconds (e.g. 500 ms). We also explore changes in the decoding accuracy as a result of increasing the duration of EEG recordings used for classification.

Two datasets are used to evaluate the performance of the proposed framework. The first dataset is collected in our lab and includes various forms of tongue/hand motor execution and imagery tasks [104]. The reason for choosing tongue movement execution task is that voluntary tongue movement is mostly preserved in patients with severe motor disorders, such as those with high spinal cord injury [105, 106], and therefore, can be utilized in BCIs to increase the number of commands in BCI-based assistive technologies for these patients. The second dataset is taken from a publicly-available source (BCI competition IV, dataset IIa) and comprises four different imagery tasks [107]. Our results demonstrate that although increasing the duration of the data used for features extraction and classification leads to enhancing the decoding accuracy, with

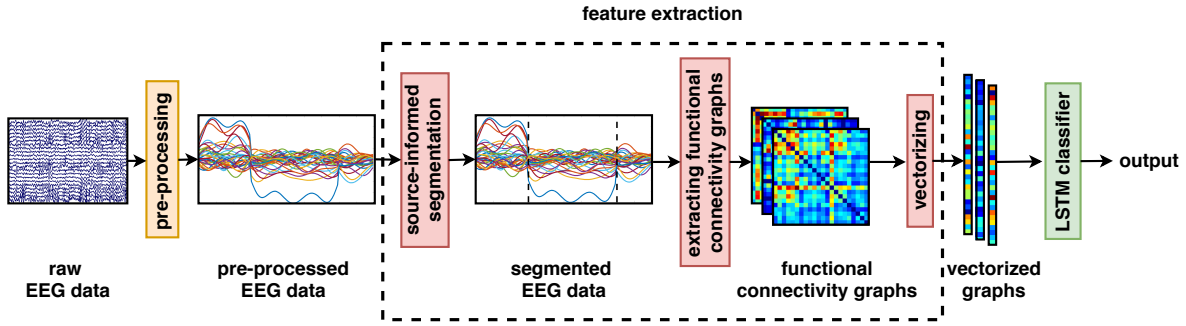

Figure 1: Overview of the proposed framework.

the duration of only 500 ms of the EEG data after the task onset, an average accuracy of 85.32% is achieved.

In summary, the contributions of this paper are as follows: 1) we present a new framework that utilizes the spatial and dynamic characteristics of brain functional networks for decoding motor tasks from EEG recordings; 2) we demonstrate, for the first time, that it is possible to achieve reasonable classification accuracy using only a few hundreds of milliseconds of data after the task onset, which can pave the path to further enhance the performance of the BCIs in terms of the required buffering lag and increasing the decoding speed; and 3) we consider classification of tongue movement execution versus hand/tongue movement imagery, which offers the possibility of increasing the number of commands in BCIs.

The rest of the paper is organized as follows: the proposed methods for feature extraction and classification of EEG data are presented in Section 2. In Section 3, the experimental paradigms and data collection procedures are described. Classification results and discussions are presented in Sections 4 and 5, respectively, and the paper is concluded in Section 6.

2. Proposed Method

A functional network corresponds to a set of brain regions that exhibit correlation to a common time-course, suggesting that they are collaborating functionally when the brain is at rest or when it is engaged in executing a task [108]. It is also now known that functional networks are dynamic, *i.e.*, they sustain their inner-connectivity for short intervals of time [17, 18]. As will be discussed here, our proposed novel feature extraction/classification framework uses functional connectivity networks as well as their dynamics, to enable the possibility of early decoding of EEG signals. An overview of the proposed framework is illustrated in Figure 1. We consider a LSTM classifier to take advantage of the information contained in the dynamics of the extracted features. In what follows, we provide details for each step in the proposed framework.

2.1. Proposed Feature Extraction Framework

The proposed feature extraction framework is comprised of two main steps: first, the pre-processed EEG data is segmented into quasi-stationary intervals, and then functional networks in each segment are localized and the corresponding graphs are constructed, which will then be used as features for the LSTM classifier.

2.1.1. EEG Segmentation The first step of feature extraction uses our recently developed source-informed segmentation algorithm [101]. The main objective of this step is to find intervals in the EEG recordings during which "*the spatial distribution*" of the cortical functional networks stays quasi-stationary. In other words, this step detects the time points in the EEG data, at which there are changes in the location of cortical networks. Therefore, this segmentation approach provides a functionally-relevant means for segmenting EEG data, which is different from the commonly-practiced model-based (e.g. autoregression) and metric-based (e.g. change point detection) segmentation approaches.

The details of the source-informed segmentation algorithm is presented in [101], and the algorithm was utilized in [109, 102, 103, 110, 111]. Briefly, this segmentation technique employs singular value decomposition (SVD) along with a reference/sliding window approach to identify targeted time intervals in the EEG data. In [101] we have proved that the most significant left singular subspace of the EEG data captures the "*spatial locality*" features of the cortical functional networks and can be used as a feature space in the segmentation algorithm. Therefore, a significant change in this span of the feature space, along the time axis, would indicate a change in the spatial distribution of the cortical functional networks. Using a reference/sliding window approach, this feature space can be dynamically extracted. The segment boundaries are detected by statistically comparing the residual error resulting from projecting the block of EEG data matrix under a reference window, on one hand, and that under a sliding window, on the other hand, onto the feature subspace [101]. It is worth mentioning that this segmentation algorithm is performed without using source localization methods, and uses the information from all EEG channels to detect the boundaries of the segments.

2.1.2. Functional Connectivity Graphs The second step of the feature extraction involves identifying the functional networks sustaining their connectivity during each identified segment and calculating the corresponding graphs. Since the nodes of these networks are taken to be the EEG electrodes, the problem of volume conduction needs to be addressed [112, 113]. For this purpose, the surface Laplacian operator [114, 115] is applied to the EEG data in order to minimize channel coupling. The segment-wise average value of each EEG channel is then removed, in order to allow the next step to focus on the temporal patterns of the activities, rather than the intensities, of these channels.

Towards identifying the functional networks forming during a given segment, we

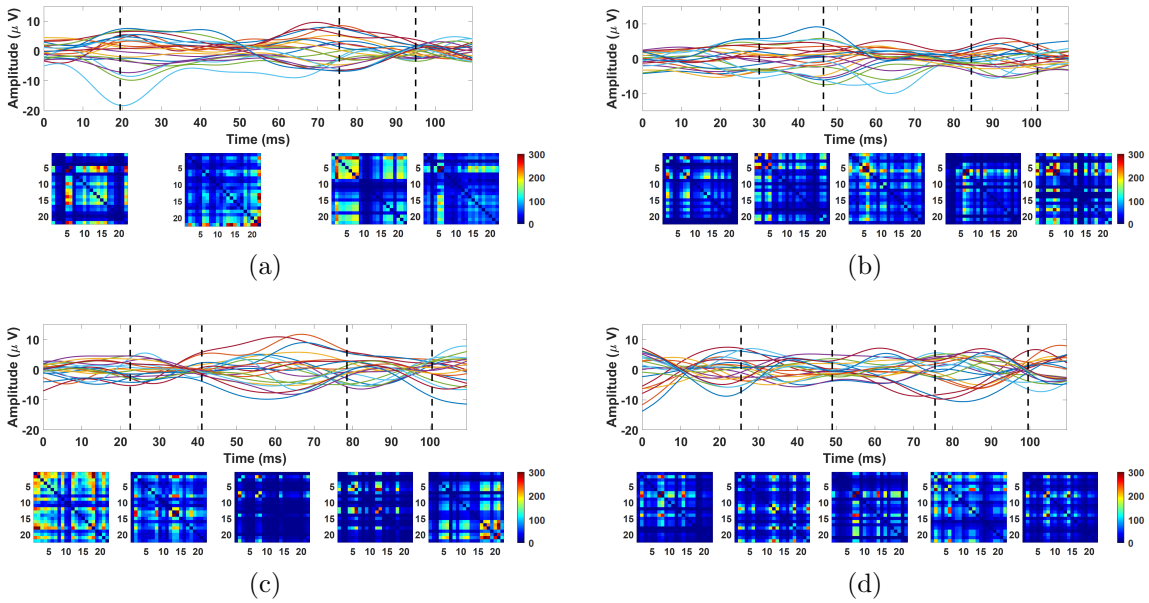

Figure 2: Segmentation and extracted color-coded functional connectivity matrices for each segment of randomly selected trials from (a):left hand motor imagery, (b): right hand motor imagery, (c): both feet motor imagery, and (d): tongue motor imagery of BCI Competition IV-IIa dataset. As can be seen, across classes of motor movement tasks, there are variations in the number and the duration of identified segments, as well as in patterns of constructed graphs.

first note that each of these networks is characterized by a distinct time-course with which the involved nodes show high correlation. Here, we use low-rank SVD to recover a minimum mean square error (MMSE) estimate of the zeros-mean channel activities conforming to these time-courses, thus, to their associated networks. For more details about this approach refer to [102]. The functional connectivity graph that captures the networks forming during that segment can finally be calculated as the correlation matrix among the estimated channel activities.

To illustrate an example of the outcome of the proposed methods, we applied the proposed segmentation and functional connectivity graph extraction algorithms to 4 randomly selected trials from the BCI Competition IV-IIa dataset (see Section 3 for more details about the experimental paradigm). Each trial was taken from one class of motor imagery (left hand, right hand, both feet, and tongue). The results for 110 ms are shown in Figure 2 as examples. It can be seen that, the length and the number of the segments, as well as the extracted graphs are different for each class, further suggesting that these features can be utilized to differentiate various forms of motor-movement classes.

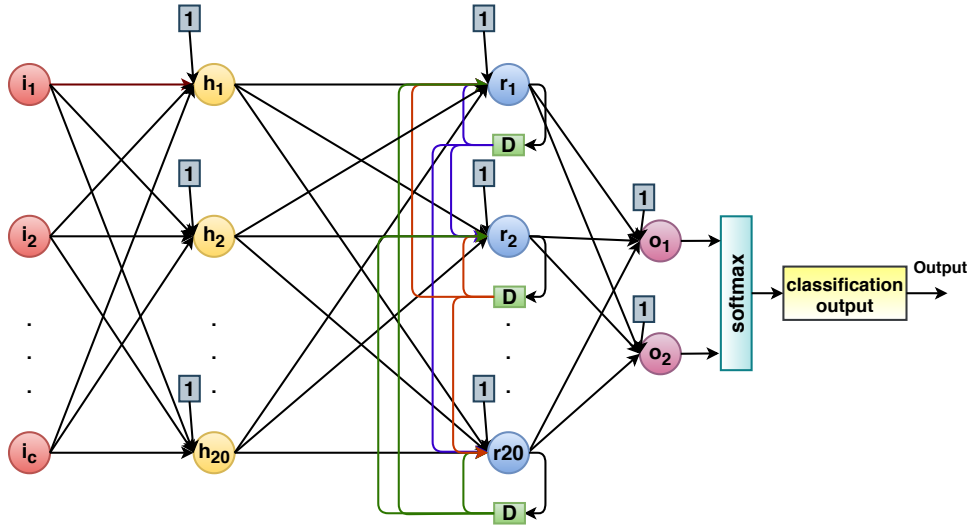

Figure 3: The structure of the LSTM classifier. Colors indicate connections from different delay units to other nodes.

2.2. Classification Scheme

Due to the dynamic nature of the brain, it is important to consider the information contained in the temporal sequence of the extracted features from identified segments. We address this point by employing a LSTM classifier. The input to these classifiers are variable-length temporal sequences of connectivity graph-based vectors. The variation in the lengths of these sequences comes from the variation in the number of the identified segments, spanning any fixed time interval.

The structure of the classifier is shown in Figure 3. A neural network with three hidden layers is used: a fully-connected layer consisting of 20 neurons, an LSTM layer consisting of 20 neurons with a single-step delay feedback loop around the second hidden layer, and another fully-connected layer consisting of 2 neurons. These layers are followed by *softmax* and classification layers. An overall classification decision is made by the neural network after it processes each segment in the sequence of dynamic functional connectivity graphs.

3. Experimental Procedure

To evaluate the performance of the proposed method, two datasets have been used. The first dataset was collected in our lab and the second dataset was available from the BCI Competition IV-IIa. Detailed descriptions of the experimental paradigms for each dataset are provided in this section.

Dataset 1: Eight healthy, right-handed volunteers (5 males and 3 females) aged between 20 and 35, participated in the study. Written informed consents approved by Rutgers' Institutional Review Board (IRB) were obtained prior to experiments. Subjects were seated in a comfortable chair with a display in front of them as shown in Figure

Figure 4: Experimental setup for Dataset 1.

4. The experiment included 3 blocks of dictated motor execution tasks and 3 blocks of dictated motor imagery tasks separated by short breaks. On average each block took approximately 7.5 minutes. In execution/imagery blocks, subjects were instructed to *move/visualize moving* their tongue upward or downward or *squeeze/visualize squeezing* their left or right hand if they saw an arrow pointing up, down, left, or right, respectively. The direction of movement, using an arrow, was shown for 1 s, followed by a diamond stimulus which was shown for 2 s. Subjects were instructed to perform motor execution or imagery only after they saw the diamond stimulus and to continue until it disappeared. The inter-trial interval was set to $2-4$ s (see Figure 5(a)). In each block, 15 trials of each class were performed (a total of 45 trials per class). EEG data was collected using a 128-channel EEG system (Brain Products), at a rate of 2000 samples/sec. We used 32 EEG channels for data analysis. The selected channels are shown in Figure 5(b). The electrodes were positioned based on the international extended $10-20$ electrode placement system.

The 2 s EEG data obtained during the presentation of the diamond stimulus, was extracted from each trial and was preprocessed using EEGLAB toolbox [116]. The data was filtered using a $[1, 50]$ Hz band-pass finite impulse response (FIR) filter, and artifacts were then removed using independent component analysis (ICA).

Dataset 2*:* This online dataset was used to conduct a performance comparison with existing work (see Section 5). The dataset provided by the Laboratory of Brain-Computer Interfaces, Graz University of Technology have been used in several BCI papers. The EEG data was collected from 9 right-handed subjects using 22 Ag/AgCl electrodes (Figure 6(b)) and 3 EOG channels, at a rate of 250 Hz. The data was collected in two sessions on different days. Each session comprised 6 runs with short breaks between blocks. During each run, the subjects were asked to perform four motor imagery tasks including the imagination of movement of the left hand, right hand, both

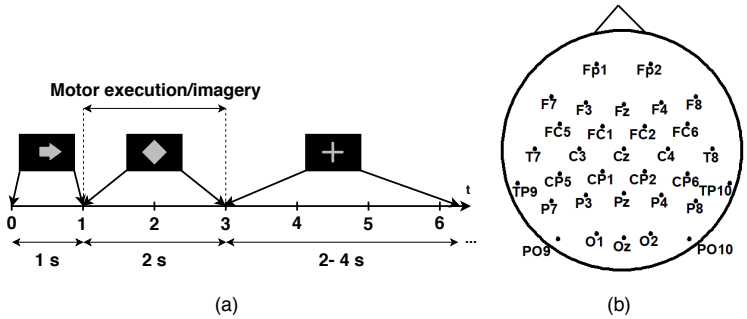

Figure 5: Dataset 1- (a): Timing scheme of a single trial. (b): EEG electrodes montage.

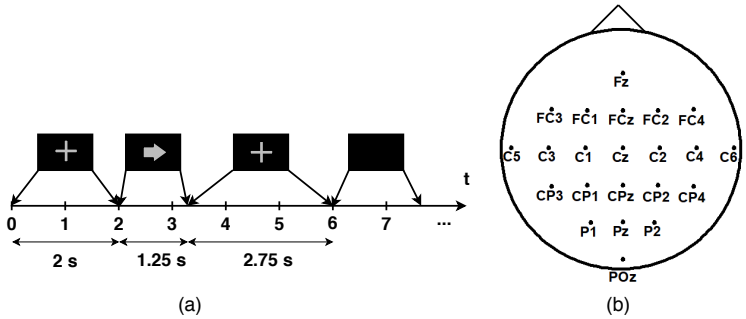

Figure 6: Dataset 2-(a): Timing scheme of a single trial. (b): EEG electrodes montage.

feet, and tongue. At the beginning of each trial, a fixation cross is shown on the black screen and a short acoustic warning tone is presented. After 2 sec, an arrow pointing to the left, right, down or up, corresponding to the motor imagery of left hand, right hand, both feet, and tongue, appears on the screen for 1.25 s, followed by a fixation cross. Subjects were asked to perform motor imagery task until the fixation cross disappears at $t = 6$ s. A short resting time was considered before starting a new trial. Each run consisted of 12 trials of each class, yielding a total of 72 trials per class in each session. A visual illustration of a single trial is shown in Figure 6(a).

Previous studies that used this dataset, have mostly considered the $[3-6]$ s window as the interval during which motor imagery tasks are performed [37, 42, 23, 25, 52, 69, 72] for the analysis. Therefore, we also extracted this 3-s motor imagery interval from each trial. Data was then preprocessed in EEGLAB toolbox [116], using a $[1, 45]$ Hz band-pass FIR filter, and ICA for removing the artifacts.

4. Results

In this section, we present the results for the performance of the proposed feature extraction/classification framework for different durations of post-stimulus EEG data. The trials were separated into three randomized groups for: training (75%), validation (10%), and testing (15%) the classification model. For Dataset 1, features extracted from 2 s post-stimulus intervals were used for training and validation. However, for testing, different time intervals of the data were used to study the early decoding capability of

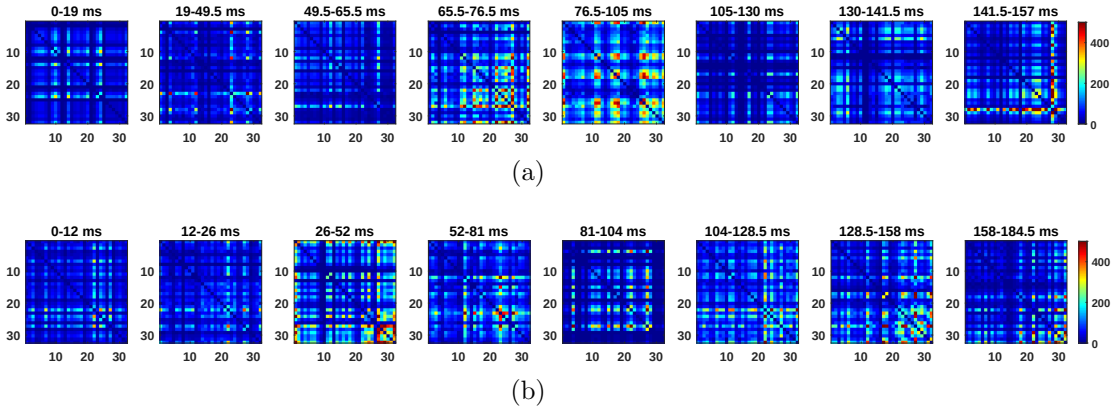

Figure 7: Extracted first 8 graph sequences of two randomly-selected trials from Dataset 1 for an exemplary subject (subject 6) (a): execution of tongue movement in the down direction, (b): imagery of right hand squeezing.

the proposed framework. The sequences of graph patterns from identified segments were passed to the classifiers and the decisions were made at the end of each segment. As the segments for different trials have different durations and ending points, to calculate the accuracy at any time instant, decisions were grouped based on the ending point of the corresponding segment into non-overlapping time bins of 100 ms duration. For example, to calculate the accuracy using the features extracted from the first 300 ms of the data, we calculate the accuracy from the segments, which end within the interval $[200, 300]$ ms.

4.1. Dataset 1*: Classification Accuracy Using 500 ms of Post-stimulus EEG Data*

For Dataset 1, 32 EEG channels (Figure 5) were used for the classification. For the segmentation step, 20 samples for both reference and decision windows were considered, which according to [101], it is a proper choice in terms of the performance of the algorithm in detecting segment boundaries. Using the 32 EEG channels, the size of the extracted functional graph matrices is 32×32. Since the extracted graphs are symmetric and include no self-loops, only the upper triangle from each graph matrix was extracted and put into a vector of size 496 (i.e., $\frac{32\times31}{2}$). The extracted graphs for an exemplary subject and two randomly-selected trials are shown in Figure 7. One can see, qualitatively, that across tasks, there are differences in the patterns of the connectivity graphs as well as in the duration of the EEG data for which the graphs were constructed as determined by the segmentation algorithm.

In this work, we focus on the classification of tongue movement execution vs tongue/hand imagery tasks. Selecting these pairs of motor execution vs imagery tasks was motivated by the fact that the tongue movement ability is often preserved in patients with motor disabilities, and its inclusion in BCIs can increase the number of control commands which is crucial in BCI-based assistive technologies. In contrast, patients in need of BCI technology usually do not possess hand movement execution ability.

Table 2: Classification accuracy results for tongue movement execution (TE) in up (U) or down (D) directions vs tongue imagery (TI) in up (U) or down (D) directions, using 500 ms after the task onset.

	U (TE) vs U (TI)	U (TE) vs D (TI)	D (TE) vs U (TI)	D (TE) vs D (TI)	**Average**
Subject 1	83.60 ± 9.59	79.93 ± 10.19	87.01 ± 8.25	80.90 ± 9.45	82.86 ± 9.39
Subject 2	84.86 ± 8.21	79.68 ± 10.27	78.95 ± 11.13	82.74 ± 9.69	81.56 ± 9.88
Subject 3	92.02 ± 6.68	94.60 ± 6.89	89.63 ± 8.24	90.12 ± 9.60	91.59 ± 7.94
Subject 4	93.61 ± 5.96	87.59 ± 7.38	94.62 ± 6.83	89.68 ± 8.19	91.37 ± 7.14
Subject 5	98.58 ± 5.67	98.70 ± 2.34	98.55 ± 3.14	98.02 ± 3.12	$\mathbf{98.46} \pm 3.78$
Subject 6	91.52 ± 8.22	90.88 ± 6.99	81.37 ± 9.58	77.25 ± 10.27	85.26 ± 8.86
Subject 7	55.87 ± 11.24	50.61 ± 12.85	58.64 ± 11.35	53.31 ± 12.18	54.36 ± 11.92
Subject 8	77.45 ± 11.32	69.65 ± 12.71	77.09 ± 11.42	66.48 ± 12.98	72.67 ± 12.13
Average	84.69 ± 8.61	81.33 ± 9.30	83.23 ± 9.13	79.81 ± 9.84	$\mathbf{82.27} \pm 9.23$

Table 3: Classification accuracy results for tongue movement execution (TE) in up (U) or down (D) directions vs imagery (HI) of left (L) or right (R) hands, using 500 ms after the task onset.

	U (TE) vs L (HI)	U (TE) vs R (HI)	D (TE) vs L (HI)	D (TE) vs R (HI)	**Average**
Subject 1	85.42 ± 10.62	85.80 ± 10.03	86.20 ± 7.85	84.13 ± 8.55	85.39 ± 9.33
Subject 2	75.48 ± 11.01	79.45 ± 10.42	69.95 ± 9.31	78.34 ± 10.48	75.81 ± 10.32
Subject 3	93.09 ± 7.68	94.94 ± 5.85	88.33 ± 8.93	91.19 ± 9.73	91.89 ± 8.18
Subject 4	95.12 ± 5.37	93.07 ± 6.93	94.05 ± 6.77	90.85 ± 9.17	93.27 ± 7.19
Subject 5	98.15 ± 3.31	98.07 ± 5.92	97.57 ± 4.38	99.14 ± 2.48	$\mathbf{98.23} \pm 4.22$
Subject 6	93.98 ± 6.35	93.05 ± 7.47	85.30 ± 9.81	82.91 ± 9.38	88.81 ± 8.37
Subject 7	74.88 ± 10.60	85.68 ± 9.82	75.69 ± 11.31	80.37 ± 11.51	79.16 ± 10.83
Subject 8	74.301 ± 12.18	72.69 ± 11.26	67.65 ± 12.09	65.52 ± 12.31	70.04 ± 11.97
Average	86.30 ± 8.90	87.84 ± 8.70	83.09 ± 9.10	84.06 ± 9.62	$\mathbf{85.32} \pm 9.09$

Therefore, discrimination of hand motor execution tasks vs tongue/hand motor imagery tasks was not considered in this study.

The accuracy, using the first 500 ms of the EEG data for classifying tongue movement execution vs tongue imagery (in various directions), and for classifying tongue movement execution vs hand movement imagery (in various directions), for all subjects, and averaged across subjects are summarized in Tables 2 and 3, respectively.

As expected, the accuracy results are subject-dependent. For Subject 5, the average accuracy for all classes was higher than 97%, while for subjects 1, 3, 4, and 6, the average accuracy results for different classes were above 80%. However, the average accuracy for tongue movement execution vs tongue imagery for subject 7 was around the chance level, which could be an outlier. Overall, average accuracy results of 82.27% and 85.32% were achieved for tongue movement execution vs tongue imagery, and tongue movement execution vs hand movement imagery tasks, respectively, across all subjects, which shows that the discrimination between tasks can be obtained within 500 ms of task onset using the proposed framework.

Table 4: Dataset 1- Classification accuracy results averaged across all subjects, for tongue movement execution (TE) vs tongue imagery (TI), and for tongue movement execution (TE) vs hand movement imagery (HI), at different post-stimulus instants.

Duration (ms)	500	700	1000	1500	1900
TE vs TI	82.27 ± 9.23	84.44 ± 8.49	85.39 ± 8.66	87.26 ± 8.45	87.35 ± 8.39
TE vs HI	85.32 ± 9.09	87.64 ± 8.64	89.08 ± 8.51	90.01 ± 8.32	90.48 ± 8.46

4.2. Dataset 1: Effects of Increasing the Time Duration of the EEG Data on the Classification Accuracy

To this point, we only considered the classification problem using the $[0 - 500]$ ms of EEG recordings where time 0 is the movement execution/imagery task onset. To study the effects of the duration of the EEG data used for the classification, on the accuracy results, the classification was performed for graph features extracted from different time intervals. The accuracy results for tongue movement execution vs tongue imagery, and for tongue movement execution vs hand movement imagery are plotted in Figures. 8 and 9, respectively.

Considering these plots, it can be concluded that for most subjects, using the proposed approach, the accuracy reaches to its high levels for EEG durations of $500 - 1000$ ms, except for Subject 5, for whom the highest accuracy was achieved in less than 500 ms.

To provide a comparison, the average accuracy results of the LSTM classifier across all subjects at different post-stimulus instants of 500, 700, 1000, 1500, and 1900 ms are summarized in Table 4. These results suggest that using longer duration of recordings leads to some improvements in the classification accuracy. However, comparing the average accuracy obtained within 500 ms to that obtained within 1900 ms, shows that despite using about 4 times of data for decision-making, the average classification accuracy results have only improved by around 5%. Therefore, it is reasonable to use 500 ms of the data for the decision-making process, which will result in less buffering and computational lag, and increasing the speed.

4.3. Significance of Considering the Dynamics of the Functional Connectivity Graphs on Classification Performance

To further emphasize the importance of including the dynamics contained within the sequence of the extracted features, we also considered a non-dynamic artificial neural network (ANN) classifier. In contrast to LSTM, the ANN classifier is incapable of taking advantage of the information conveyed by the sequencing of the feature vectors. We used an ANN model with two fully-connected hidden layers consisting of 20 neurons. The average classification results achieved at 500 ms using the ANN classifier for different classes of tongue movement execution vs imagery, and tongue movement execution vs hand movement imagery, compared to the accuracy results achieved from the LSTM

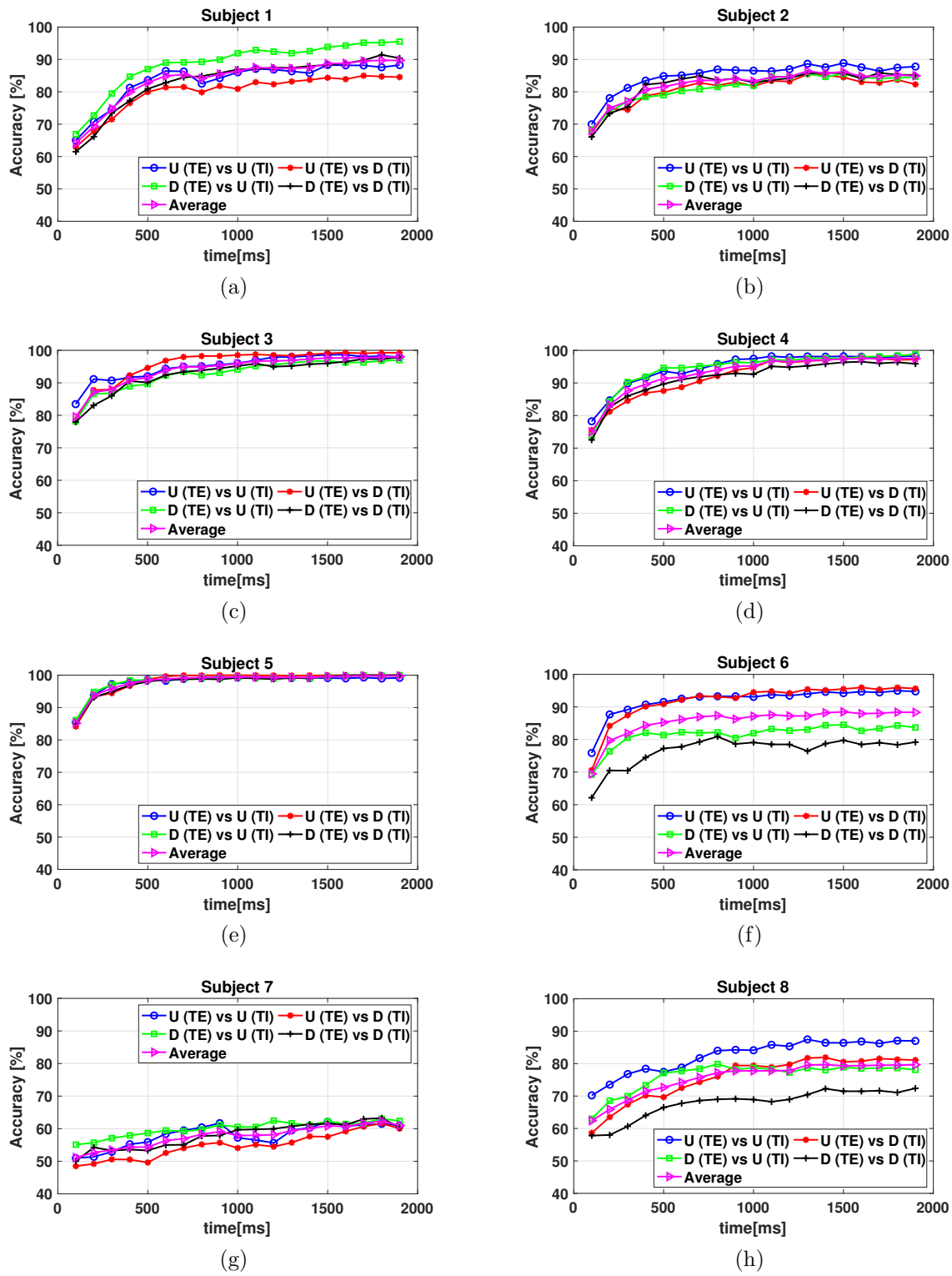

Figure 8: (a)-(h): Classification accuracy of tongue movement execution (TE) in up (U) or down (D) directions vs tongue imagery (TI) in up (U) or down (D) directions for all subjects.

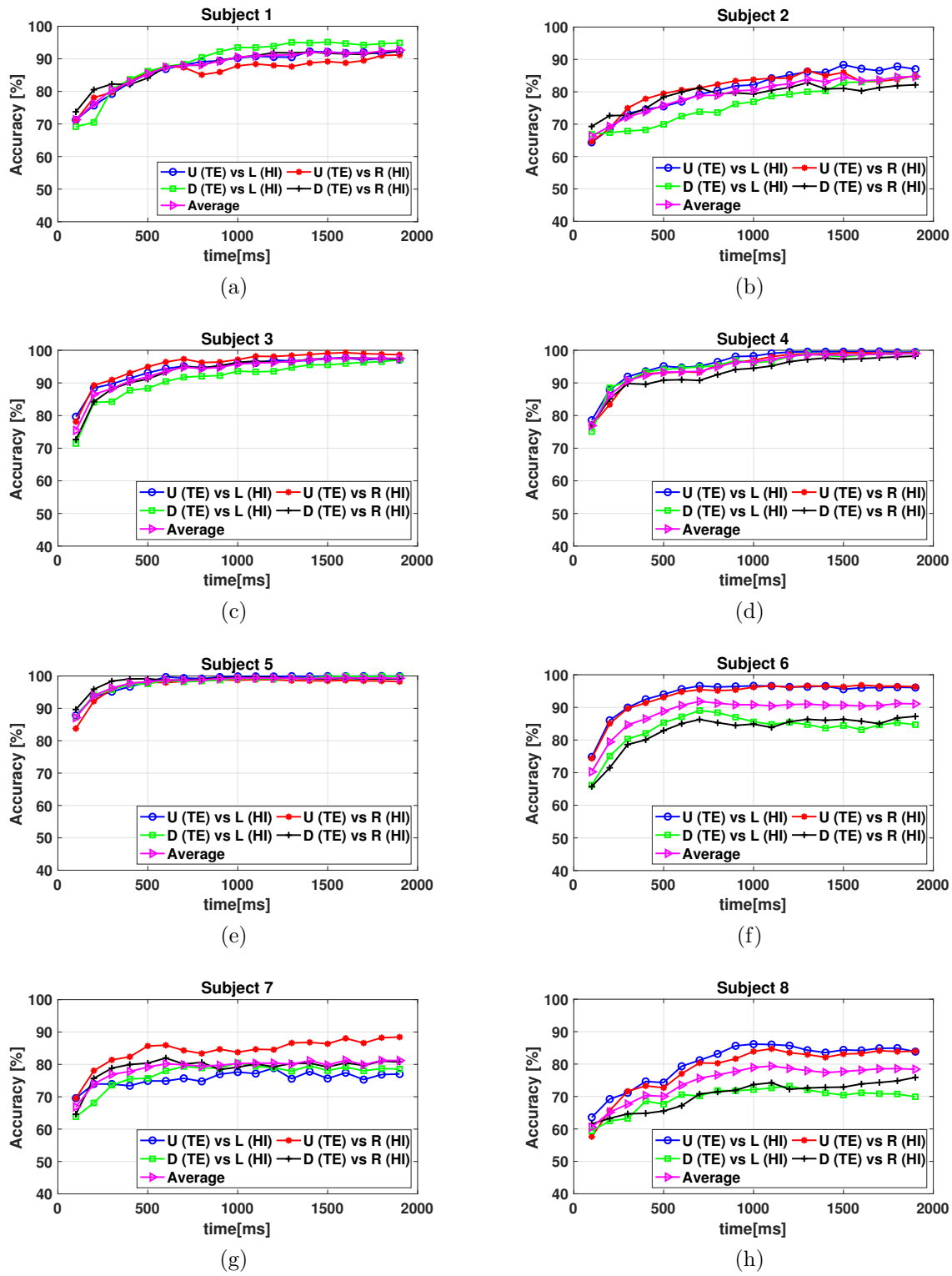

Figure 9: (a)-(h): Classification accuracy of tongue movement execution (TE) in up (U) or down (D) directions vs imagery (HI) of left (L) or right (R) hands for all subjects.

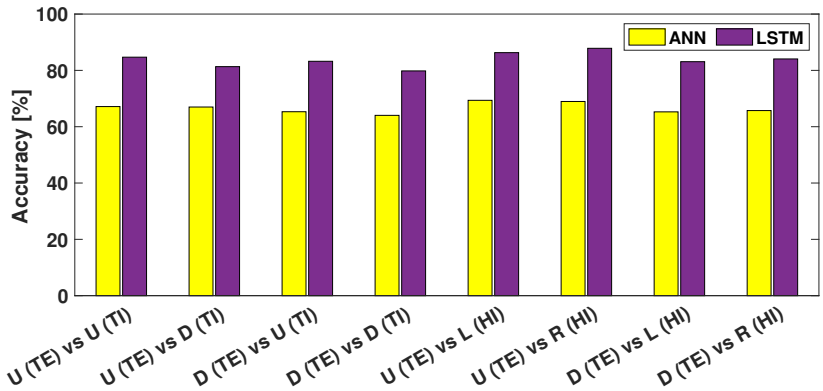

Figure 10: Average classification accuracy results, for 500 ms of the EEG data, for different classes of tongue movement execution (TE) vs imagery (TI) and tongue movement execution (TE) vs hand movement imagery (HI) using ANN and LSTM classifiers.

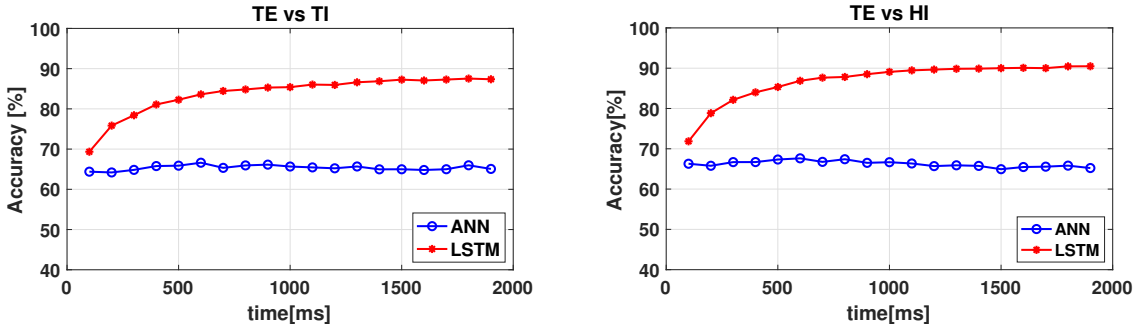

(a) (b)

Figure 11: Average classification accuracy results for tongue movement execution (TE) vs (a): tongue movement imagery (TI) and (b): hand movement imagery (HI) using ANN and LSTM classifiers.

classifier are presented in Figure 10. As can be seen, the average classification accuracy using the LSTM classifier is about 18% higher than the accuracy results achieved from the ANN classifier (across classes), which confirms that the inclusion of the information that lies in the temporal sequence of extracted features plays an important role in improving the performance.

Additionally, from Figure 11, one can see that, for the ANN-based classifier, the average classification accuracy does not improve as time goes by. This is caused by the exclusion of the temporal information of the sequence in the ANN classifier, thus, discriminating different tasks is only based on the spatial information of functional connectivity graphs. In summary, these results demonstrate the significance of considering the dynamics of the functional connectivity graphs for discriminating motor tasks.

5. Discussion

There has been significant interest in studying task-based or resting-state brain's functional connectivity in healthy and patient subjects, which has resulted in new understanding about the brain function as well as the mechanisms underlying brain-related disorders [117, 118, 119, 120, 121, 122, 123, 124, 125, 17, 126]. In BCIs, functional connectivity measures have been employed as features to discriminate various tasks [28, 26, 27, 22, 23]. This approach is in contrast to most of the BCI algorithms in which features are typically extracted from individual EEG electrodes. Previous studies suggest that using features from individual EEG electrodes may not provide enough information to discriminate motor tasks in specific groups of patients with motor disabilities [127]. For example, it has been shown that there exist differences in the band power patterns corresponding to motor imagery tasks across stroke patients with different location of lesion [128, 129, 130], and therefore, combining various features have been suggested as a solution to improve the classification performance [129]. Since performing tasks relies on the interactions among various brain regions, it is intuitive to consider functional connectivity-based characteristics rather than using features from isolated regions/electrodes for the purpose of discriminating intended tasks.

Brain is known to be a dynamical system in which interactions among different regions are time-varying [131, 17, 132, 133, 134]. These interactions are transient and rapid (*i.e.* established on the millisecond time scale). Accordingly, it has been suggested that studying the functional connectivity networks along with their temporal variations over the course of the task execution provide a better understanding of the brain function compared to the case of studying functional connectivity networks in a static framework, which is incompatible with the dynamic nature of the brain. Based on these facts, in this paper, we presented a novel feature extraction/classification framework which utilizes dynamic functional connectivity networks to decode the motor execution/imagery tasks. Furthermore, we aimed to reduce the time interval required to achieve reasonable accuracy.

The proposed framework includes segmentation of the EEG data into variable-length time intervals where the functional connectivity networks remain quasi-stationary, and then constructing the functional connectivity graphs for each identified segment. It is worth to mention that most of the previously-presented methods (such as dynamic time warping (DTW), or microstates) for studying the brain dynamics through EEG recordings have been based on changes in the activities that form on the scalp (sensor space)[17, 135, 136, 137]. In contrast, our novel source-informed segmentation algorithm identifies segment boundaries based on changes in the spatial characteristics of the functional networks in the cortex (source space). This makes the algorithm informed by the source space, without requiring computationally complex source localization [101].

The sequence of extracted features were passed to the LSTM classifier to take advantage of the information that lies in the temporal sequence of the constructed

connectivity graphs. The obtained classification accuracy results indicate that the proposed method can successfully discriminate tongue movement execution vs tongue (82.27%)/hand (85.32%) movement imagery tasks at only 500 ms after the task onset. These results suggest that the interactions among different brain regions evoked by motor execution/imagery tasks (*i.e.* connectivity patterns) along with their temporal dynamics within a short interval (in the order of a few hundreds of milliseconds) can provide sufficient information for solving the classification problem. Therefore, the proposed feature extraction/classification framework can be utilized to reduce the required buffering lag for the BCIs, and thereby, increasing their speed.

Our results suggest that the temporal dynamics of functional networks play key roles in early decoding capability that is offered by the proposed framework. This was highlighted by comparing the classification results achieved from two classifiers, with one (LSTM) taking both temporal dynamics and spatial information of functional connectivity graphs into account, while the other (ANN) only utilizing the spatial information. It was observed that for the ANN classifier, there was not much difference in the obtained classification accuracy results along time, while in the case of the LSTM classifier, the average accuracy results improved along the time spent after task onset (see Figure 11). These results further confirm the importance of the inclusion of the temporal information of the functional connectivity networks in achieving good classification performance within a short interval. The significance of including the temporal information can be observed as early as 100 ms after the task onset, where the average classification accuracy using LSTM is $\sim 5\%$ higher than the case of using ANN classifier. This difference increases to $16.39 - 17.99\%$ and $22.28 - 25.26\%$ for 500 and 1900 ms after the task onset, respectively. It can be concluded that the interactions among the brain regions and how they evolve over the course of the task performance contribute to discriminatory information needed to solve the classification problem.

The proposed method was employed to differentiate motor execution vs imagery tasks. The similarities and differences in connectivity patterns of motor execution and imagery tasks were investigated in [138, 139, 140, 123]. In [138], coupling patterns among occipital and motor regions in the beta frequency band were reported to be different during hand movement execution and imagery. The betweenness centrality (BC) feature of functional connectivity graphs was used in [139] to study the functional connectivity networks corresponding to movement execution and imagery of finger tapping. The results revealed that the key nodes for motor execution and imagery tasks are located in different areas. In [140] and [123] functional connectivity analysis based on ERS/ERD and phase synchronization showed similar connectivity patterns among contralateral brain regions for movement execution and imagery of finger tapping [140], and foot and hand [123]. In [141], the results of effective connectivity networks associated with finger tapping execution and imagery indicated that the coupling strength of the feedforward network from dorsolateral prefrontal cortex to premotor cortex was greater during motor execution tasks than to motor imagery tasks, whereas the coupling strength of the feedforward network from premotor cortex to supplementary motor area

and the feedback network from the primary motor cortex to premotor cortex were higher for motor imagery tasks. Functional connectivity networks corresponding to hand movement execution and imagery were investigated over two frequency bands of μ and β using sensor-level connectivity analysis in [142]. The results suggested that increases in β-band connectivity occurred the same way in both movement execution and imagery tasks while in μ band, motor execution and imagery tasks were associated with different connectivity patterns. Considering the results of these studies, it can be concluded that depending on the analysis methods and variables that are selected as the basis of comparisons, one might observe common or different connectivity patterns among motor execution and imagery tasks. In this paper, we showed that using the proposed method, *dynamic* functional connectivity networks can provide discriminatory information corresponding to motor execution vs imagery tasks. Frequency-specific analysis can bring more insights into understanding how different EEG frequency bands contribute in differentiating among motor execution vs imagery tasks. We aim to investigate this problem in our future studies.

It is worth to mention that for Dataset 1, we demonstrated that tongue movement execution can be discriminated from tongue/hand movement imagery movement tasks. The importance of discriminating tongue movement execution vs other imagery tasks is that the movement of tongue is often available even in patients with severe motor disabilities. Differentiation of tongue movement from other motor imagery activities can be advantageous in BCI applications and BCI-based assistive technologies since it increases the number of control commands.

In order to compare the performance of the proposed approach with existing methods, we also applied the classification algorithm to the BCI Competition IV dataset IIa (Dataset 2), which has been commonly used in BCI studies. Features extracted from 3-s duration of motor imagery task ($[3-6]$ s interval, see Figure 6(a)) were employed for training and validation. For testing, 800 ms interval, after the motor imagery task onset, was used. The reason for selecting this duration is that when plotting accuracy graphs similar to Figures 8 and 9 for this dataset, we observed that around 800 ms a reasonable accuracy can be achieved. The classification results for differentiating various pairs of MI tasks (*i.e.* left hand vs right hand (L vs R), left hand vs both feet (L vs F), left hand vs tongue (L vs T), right hand vs both feet (R vs F), right hand vs tongue (R vs T), and both feet vs tongue (F vs T)) for all subjects are presented in Table 5. Accuracy results greater than 80% are also emphasized in bold.

As can be seen, the best accuracy results have been achieved for left hand vs tongue, and for right hand vs tongue classification cases, whereas the least accuracy results were obtained for feet vs tongue, and left hand vs right hand classification cases. One possible explanation for this observation is that the spatial and temporal patterns of the estimated functional networks could be more discriminatory among some pairs of imagery tasks as compared to others. Further exploring the characteristics of these networks can deepen our understanding of the reasons for achieving different decoding accuracy results across pairs of motor imagery tasks. Moreover, similar to the results

Table 5: Classification accuracy results for classifying various pairs of left hand (L), right hand (R), both feet (F), and tongue (T) movement imagery tasks using 800 ms after the task onset for Dataset 2 (Dataset IIa from BCI competition IV).

SUB	L vs R	L vs F	L vs T	R vs F	R vs T	F vs T
A01	59.91 ± 6.88	$\mathbf{80.62} \pm 6.45$	$\mathbf{86.12} \pm 4.92$	$\mathbf{81.49} \pm 6.95$	$\mathbf{91.56} \pm 4.46$	55.18 ± 6.36
A02	56.24 ± 6.62	72.87 ± 7.07	68.56 ± 7.45	75.35 ± 6.66	74.06 ± 6.92	60.39 ± 6.25
A03	77.26 ± 6.01	76.08 ± 6.88	$\mathbf{86.47} \pm 5.24$	$\mathbf{86.21} \pm 5.37$	$\mathbf{92.19} \pm 3.70$	70.57 ± 6.95
A04	58.88 ± 7.48	63.23 ± 7.01	64.91 ± 6.98	68.84 ± 8.17	63.59 ± 6.53	60.92 ± 7.61
A05	56.88 ± 6.39	52.03 ± 4.84	53.49 ± 5.96	53.44 ± 5.77	55.07 ± 6.36	51.03 ± 5.86
A06	60.42 ± 8.21	60.67 ± 6.98	62.31 ± 7.24	56.23 ± 7.56	60.21 ± 7.90	58.59 ± 7.12
A07	59.48 ± 6.06	$\mathbf{88.13} \pm 4.98$	$\mathbf{85.97} \pm 5.54$	$\mathbf{83.22} \pm 5.29$	$\mathbf{84.80} \pm 6.43$	72.74 ± 6.53
A08	$\mathbf{82.50} \pm 5.44$	69.69 ± 7.50	$\mathbf{85.81} \pm 5.48$	76.91 ± 6.91	$\mathbf{81.00} \pm 5.85$	76.90 ± 5.75
A09	$\mathbf{84.87} \pm 5.64$	$\mathbf{86.04} \pm 5.72$	$\mathbf{94.13} \pm 3.69$	65.82 ± 6.75	74.31 ± 7.09	$\mathbf{80.66} \pm 6.60$
Average	66.27 ± 6.68	72.19 ± 6.45	76.42 ± 5.95	71.94 ± 6.67	75.20 ± 6.26	65.22 ± 6.59

obtained from Dataset 1, the results for this dataset were also subject-dependent. The accuracy results for subjects 1, 3, 7, 8, and 9 were higher than others, while the accuracy results for subjects 5 and 6 were mostly on the low end. Although the accuracy results for other subjects were satisfactory, inclusion of these two subjects, has reduced the overall obtained averaged accuracy across subjects.

Table 6 summarizes the classification results for some of the recent work that have used Dataset 2 along with the required duration of the data that was used to achieve these classification accuracy results. For a better comparison, here we focused on studies that had reported the results for different pairs of MI tasks. It can be seen that, in terms of the buffering lag, for this dataset, our work has used the shortest duration (800 ms) which is considerably shorter than other methods that required equal or greater than 2 s of EEG recordings to perform classification. In terms of types of extracted features, [25] and [23] are the closest to our work for comparison as they have employed functional connectivity-based features, albeit without considering the dynamics. Compared to these two studies, it can be observed that our work has led to better accuracy results in most cases of MI classification (while using only 800 ms of the EEG data), further suggesting the importance of the inclusion of dynamic information for discriminating motor imagery tasks. In terms of classifiers, similar to our case, [38] has used LSTM, however, the extracted features are channel-based and are computed in the time domain. The reported classification accuracy results from this method using 3 s duration of EEG recordings are comparable to the results of our proposed method from 800 ms data. Furthermore, [38] also shows results using a deep learning classification algorithm based on Restricted Boltzmann Machines (RBM) [80], which are lower for all pairs of MI tasks as compared to our results. In [143], a method for reducing the effects of noisy trials was used, which has resulted in improved classification performance, although the buffering lag has not been reported. In our case, we had only considered basic preprocessing steps (filtering and ICA). The possibility of achieving higher accuracy results with more advanced preprocessing methods such as those proposed in [143] requires further

Table 6: Comparison of classification accuracy results and the required time, of the proposed method and existing work using Dataset 2 (Dataset IIa from BCI competition IV)

Ref.	Year	Duration (s)	Feature Type	Classifier	Accuracy (%)					
					L vs R	L vs F	L vs T	R vs F	R vs T	F vs T
[37]	2016	3	Channel-based	SVM	74.92	-	-	-	-	-
[25]	2016	3.5	Functional Connectivity	SVM	64.27	-	-	-	-	-
[80, 38]	2017	3	Channel-based	RBM	64.60	65.60	61.90	66.80	70.20	64.60
[143]	2017	unknown	Channel-based	MNN	79.52	83.19	84.64	81.44	83.40	78.64
[52]	2018	2	Channel-based	SVM	82.50	-	-	-	-	84.00
[42]	2018	2	Channel-based	MDRM	79.93	85.50	84.30	85.43	83.75	74.78
[38]	2018	3	Channel-based	LSTM	74.80	74.20	72.50	76.30	74.30	79.60
[55]	2019	2	Channel-based	MDRM	80.98	-	-	-	-	-
[23]	2019	3	Functional Connectivity	LS	71.00	74.00	74.00	71.00	74.00	65.00
This work	-	**0.8**	Functional Connectivity	LSTM	66.27	72.19	76.42	71.94	75.20	65.22

investigation. In [37, 52, 42, 55] channel-based features extracted from 2 or 3 s duration of EEG data were employed for classification of motor imagery tasks. In [37], an adaptive learning method is used, which continuously monitors the features extracted from EEG data to detect the shifts in their probability distribution and adaptively updates the classifier during the testing phase. Despite the good classification results reported in this study, implementing this method is not computationally efficient due to the procedures involved in the decoding algorithm. In [52] and [42], features are extracted from specific EEG frequency bands. In [52], both the filter bandwidth and the time window used for feature extraction were optimized, which resulted in enhanced classification accuracy. However, in our work, we did not consider band-specific results. It would be interesting to investigate whether employing frequency-specific dynamic functional connectivity networks as features will improve the accuracy results in the future. Finally, in [55], a Riemannian-based approach is used which incorporates inter-subject data to reduce the dimensionality of the covariance matrices through regularization techniques. Including the inter-subject data in our proposed dynamic functional connectivity-based method can be an interesting topic for the future studies.

In summary, it can be concluded that although some of the studies in Table 6 have reported higher classification accuracy results as compared to our case, we have shown that within a notably shorter duration, reasonable classification accuracy can be achieved using our proposed method. Our early decoding method is well-suited for applications that require decoding the user's intentions within a short interval after the onset of the task, while other methods could be more preferable if higher decoding accuracy is required and the duration of the buffering lag is not a concern.

To the best of our knowledge, this is the first study that demonstrates the possibility of early decoding of motor tasks in BCIs from EEG recordings. There are a few limitations in this study. Here, we have performed off-line processing and classification of EEG data. In order to use this method in real-time BCIs, a framework for a real-time implementation of the feature extraction algorithm should be developed. With the current progress in the development of computational hardware and processing units,

this seems to be achievable in the near future. Moreover, previous studies on MI-based EEG classification [144, 145, 146, 58] have demonstrated the role of specific EEG frequency bands in the classification of MI tasks. We did not incorporate frequency decomposition here. An extension of this work could be focused on the extraction of functional networks from different EEG frequency bands to investigate the significance of each frequency band in addressing the early decoding problem. Additionally, we only considered basic FIR filtering and artifact removal using ICA. The performance of the proposed method can further be improved by incorporating noise and artifact reduction techniques in the algorithm and/or utilizing mechanisms to detect and remove noisy trials as suggested in [143].

It is also worth mentioning that although we have verified the early-decoding effectiveness of the proposed approach using two different datasets, the collected data belonged to healthy groups. For the purpose of implementing BCI-based assistive technologies for patients, testing the proposed framework on data collected from patients would be necessary. Moreover, in this work, we considered the decoding problem for movement- related tasks. However, the proposed framework can also be applied to other tasks, such as P300 and cognitive tasks, to evoke brain activities in BCIs. Implementing the proposed method for early decoding of other mental activities from EEG recordings may offer the ability to improve the speed and practicality of the BCIs that are based on these tasks.

6. Conclusions

This paper introduced a new feature extraction method based on dynamic functional connectivity networks for early decoding of EEG signals. The proposed method comprised of two steps: first, segmenting the EEG data into quasi-stationary temporal blocks during which functional networks sustain their connectivity, and second constructing functional connectivity graphs for each identified segment. An LSTM classifier was then employed for the classification due to its advantageous utilization of the contained memory cell which allowed for processing a sequence of features.

The proposed method enabled us to differentiate among tongue movement execution vs tongue or hand movement imagery tasks within a short interval of only a few hundreds of milliseconds with good accuracy. These results indicated, for the first time, that the required duration of EEG data on a given trial for decoding motor execution and imagery tasks, can be significantly reduced compared to existing methods, suggesting that this framework is an efficient approach for improving the speed of BCIs. Additionally, we showed that the early decoding capability relied on both spatial and temporal information of functional connectivity networks that were captured by using the proposed feature extraction method and utilizing the LSTM classifier.

This study was the first step in addressing the early classification problem from EEG data. The extension of the proposed method for band-specific early decoding, and multi-class problems are considered as our future work.

Acknowledgment

The authors would like to acknowledge the support from NSF (Award 1841087), Siemens, and DARPA. The authors would also like to thank Jennifer Huang for her help in EEG data collection.

References

[1] Lotte F, Congedo M, Lécuyer A, Lamarche F and Arnaldi B *Journal of Neural Engineering* **4** R1
[2] Lotte F, Bougrain L, Cichocki A, Clerc M, Congedo M, Rakotomamonjy A and Yger F *Journal of Neural Engineering* **15** 031005
[3] Aggarwal S and Chugh N 2019 *Array* **1** 100003
[4] Sun L, Feng Z, Lu N, Wang B and Zhang W 2019 *Expert Systems with Applications* **131** 9–19
[5] Duan L, Bao M, Cui S, Qiao Y and Miao J 2017 *Cognitive Computation* **9** 758–765
[6] Wang H, Zhang Y *et al.* 2016 *Measurement* **86** 148–158
[7] Taran S and Bajaj V 2018 *Neural Computing and Applications* 1–8
[8] Taran S, Bajaj V, Sharma D, Siuly S and Sengur A 2018 *Measurement* **116** 68–76
[9] Shan H, Xu H, Zhu S and He B 2015 *Biomedical engineering online* **14** 93
[10] Soman S *et al.* 2015 *Applied Soft Computing* **30** 305–318
[11] Ai Q, Chen A, Chen K, Liu Q, Zhou T, Xin S and Ji Z 2019 *Journal of neural engineering* **16** 026032
[12] Ibáñez J, Serrano J I, del Castillo M D, Minguez J and Pons J L 2015 *Medical & biological engineering & computing* **53** 1201–1210
[13] Olivas-Padilla B E and Chacon-Murguia M I 2019 *Applied Soft Computing* **75** 461–472
[14] Edelman B J, Baxter B and He B 2016 *IEEE Transactions on Biomedical Engineering* **63** 4–14
[15] Komijani H, Parsaei M R, Khajeh E, Golkar M J and Zarrabi H 2017 *Neural Computing and Applications* 1–12
[16] Li Y, Zhang X R, Zhang B, Lei M Y, Cui W G and Guo Y Z 2019 *IEEE Transactions on Neural Systems and Rehabilitation Engineering*
[17] Karamzadeh N, Medvedev A, Azari A, Gandjbakhche A and Najafizadeh L 2013 *NeuroImage* **66** 311–317
[18] Allen E, Damaraju E, Eichele T, Wu L and Calhoun V D 2018 *Brain topography* **31** 101–116
[19] Gonzalez-Castillo J and Bandettini P A 2018 *Neuroimage* **180** 526–533
[20] Bastos A M and Schoffelen J M 2016 *Frontiers in systems neuroscience* **9** 175
[21] Lu C F, Teng S, Hung C I, Tseng P J, Lin L T, Lee P L and Wu Y T 2011 *Clinical Neurophysiology* **122** 1569–1579
[22] Li F, Peng W, Jiang Y, Song L, Liao Y, Yi C, Zhang L, Si Y, Zhang T, Wang F *et al.* 2019 *International journal of neural systems* **29** 1850016
[23] Rodrigues P G, Stefano Filho C A, Attux R, Castellano G and Soriano D C 2019 *Medical & biological engineering & computing* **57** 1709–1725
[24] Tang M, Lu Y and Yang L 2019 *IEEE Transactions on Neural Systems and Rehabilitation Engineering* **27** 643–651
[25] Gonuguntla V, Wang Y and Veluvolu K C 2016 *IEEE journal of selected topics in signal processing* **10** 1284–1294
[26] Gaxiola-Tirado J A, Salazar-Varas R and Gutiérrez D 2017 *IEEE Transactions on Cognitive and Developmental Systems* **10** 776–783
[27] Stefano Filho C A, Attux R and Castellano G 2018 *Biomedical Signal Processing and Control* **40** 359–365
[28] Daly I, Nasuto S J and Warwick K 2012 *Pattern recognition* **45** 2123–2136
[29] Tiwari P, Ghosh S, Sinha R K *et al.* 2015 *Computational intelligence and neuroscience* **2015** 59

[30] Zhang R, Xiao X, Liu Z, Jiang W, Li J, Cao Y, Ren J, Jiang D and Cui L 2018 *IEEE Access* **6** 44944–44950
[31] Liao K, Xiao R, Gonzalez J and Ding L 2014 *PloS one* **9** e85192
[32] García-Laencina P J, Rodríguez-Bermudez G and Roca-Dorda J 2014 *Expert Systems with Applications* **41** 5285–5295
[33] Miao M, Wang A and Liu F 2017 *Medical & biological engineering & computing* **55** 1589–1603
[34] Zhao X, Zhang H, Zhu G, You F, Kuang S and Sun L 2019 *IEEE Transactions on Neural Systems and Rehabilitation Engineering* **27** 2164–2177
[35] Sturm I, Lapuschkin S, Samek W and Müller K R 2016 *Journal of neuroscience methods* **274** 141–145
[36] Li X, Guan C, Zhang H, Ang K K and Ong S H 2014 *Journal of neural engineering* **11** 056020
[37] Raza H, Cecotti H, Li Y and Prasad G 2016 *Soft Computing* **20** 3085–3096
[38] Wang P, Jiang A, Liu X, Shang J and Zhang L 2018 *IEEE Transactions on Neural Systems and Rehabilitation Engineering* **26** 2086–2095
[39] Ha K W and Jeong J W 2019 *Sensors* **19** 2854
[40] Kang H and Choi S 2014 *Neural Networks* **57** 39–50
[41] Gaur P, Pachori R B, Wang H and Prasad G 2019 *IEEE Sensors Journal*
[42] Gaur P, Pachori R B, Wang H and Prasad G 2018 *Expert Systems with Applications* **95** 201–211
[43] Kim Y, Ryu J, Kim K K, Took C C, Mandic D P and Park C 2016 *Computational intelligence and neuroscience* **2016** 1
[44] Zhang Y, Wang Y, Jin J and Wang X 2017 *International journal of neural systems* **27** 1650032
[45] Qiu Z, Jin J, Lam H K, Zhang Y, Wang X and Cichocki A 2016 *Neurocomputing* **207** 519–527
[46] Liu R, Wang Y, Newman G I, Thakor N V and Ying S 2017 *International journal of neural systems* **27** 1750046
[47] Feng J, Yin E, Jin J, Saab R, Daly I, Wang X, Hu D and Cichocki A 2018 *Neural Networks* **102** 87–95
[48] Luo J, Feng Z and Lu N 2019 *Biomedical Signal Processing and Control* **47** 137–144
[49] Qi F, Li Y and Wu W 2015 *a, a* **1** 1
[50] Ameri R, Pouyan A and Abolghasemi V 2016 *Neurocomputing* **218** 382–389
[51] Park S H, Lee D and Lee S G 2018 *IEEE Transactions on Neural Systems and Rehabilitation Engineering* **26** 498–505
[52] Zhang Y, Nam C S, Zhou G, Jin J, Wang X and Cichocki A 2018 *IEEE transactions on cybernetics* **49** 3322–3332
[53] Meng J, Yao L, Sheng X, Zhang D and Zhu X 2015 *IEEE transactions on biomedical engineering* **62** 227–240
[54] Tavakolan M, Yong X, Zhang X and Menon C 2016 *Journal of medical and biological engineering* **36** 12–21
[55] Singh A, Lal S and Guesgen H W 2019 *IEEE Access* **7** 46858–46869
[56] Xie X, Yu Z L, Gu Z, Zhang J, Cen L and Li Y 2018 *IEEE Transactions on Neural Systems and Rehabilitation Engineering* **26** 698–708
[57] Dai G, Zhou J, Huang J and Wang N 2019 *Journal of neural engineering*
[58] Kumar S, Sharma A and Tsunoda T 2017 *BMC bioinformatics* **18** 545
[59] Zhang Y, Zhou G, Jin J, Wang X and Cichocki A 2015 *Journal of neuroscience methods* **255** 85–91
[60] Liu Y, Zhao Q and Zhang L 2015 *International journal of neural systems* **25** 1550013
[61] Kevric J and Subasi A 2017 *Biomedical Signal Processing and Control* **31** 398–406
[62] Li Y, Wen P P *et al.* 2014 *Computer Methods and programs in Biomedicine* **113** 767–780
[63] Yong X and Menon C 2015 *PloS one* **10** e0121896
[64] Lu N, Li T, Pan J, Ren X, Feng Z and Miao H 2015 *Computers in biology and medicine* **60** 32–39
[65]
[66] Andrade M K, de Santana M A, Moreno G, Oliveira I, Santos J, Rodrigues M C A and dos Santos

W P 2020 An eeg brain-computer interface to classify motor imagery signals *Biomedical Signal Processing* (Springer) pp 83–98

[67] Luo J, Feng Z, Zhang J and Lu N 2016 *Computers in biology and medicine* **75** 45–53

[68] Dose H, Møller J S, Iversen H K and Puthusserypady S 2018 *Expert Systems with Applications* **114** 532–542

[69] Nguyen C H and Artemiadis P 2018 *Neurocomputing* **275** 1871–1883

[70] Lu N and Yin T 2015 *Journal of neuroscience methods* **249** 41–49

[71] Amin S U, Alsulaiman M, Muhammad G, Bencherif M A and Hossain M S 2019 *IEEE Access* **7** 18940–18950

[72] Hersche M, Rellstab T, Schiavone P D, Cavigelli L, Benini L and Rahimi A 2018 *arXiv preprint arXiv:1806.06823*

[73] Xu P, Liu T, Zhang R, Zhang Y and Yao D 2014 *Biomedical Signal Processing and Control* **10** 289–295

[74] Fu R, Tian Y, Bao T, Meng Z and Shi P 2019 *Journal of medical systems* **43** 169

[75] Chatterjee R, Moitra T, Islam S H, Hassan M M, Alamri A and Fortino G 2019 *Future Generation Computer Systems*

[76] Malan N S and Sharma S 2019 *Computers in biology and medicine* **107** 118–126

[77] Hsu W Y 2014 *Clinical EEG and neuroscience* **45** 163–168

[78] Wang J, Feng Z, Lu N, Sun L and Luo J 2018 *Biomedical Signal Processing and Control* **46** 10–17

[79] Hsu W Y 2014 *International Journal of Fuzzy Systems* **16**

[80] Lu N, Li T, Ren X and Miao H 2017 *IEEE transactions on neural systems and rehabilitation engineering* **25** 566–576

[81] Kee C Y, Ponnambalam S and Loo C K 2017 *Neural Computing and Applications* **28** 2051–2062

[82] Peterson V, Wyser D, Lambercy O, Spies R and Gassert R 2019 *Journal of neural engineering* **16** 016019

[83] Hsu W C, Lin L F, Chou C W, Hsiao Y T and Liu Y H 2017 *International Journal of Fuzzy Systems* **19** 566–579

[84] Miao M, Zeng H, Wang A, Zhao C and Liu F 2017 *Journal of neuroscience methods* **278** 13–24

[85] Zhang Y, Wang Y, Zhou G, Jin J, Wang B, Wang X and Cichocki A 2018 *Expert Systems with Applications* **96** 302–310

[86] Chen S, Luo Z and Gan H 2018 *Neural Computing and Applications* **29** 857–863

[87] Nguyen T, Khosravi A, Creighton D and Nahavandi S 2015 *Expert Systems with Applications* **42** 4370–4380

[88] Ma Y, Ding X, She Q, Luo Z, Potter T and Zhang Y 2016 *Computational and mathematical methods in medicine* **2016**

[89] Fang Y, Chen M and Zheng X 2015 *Neurocomputing* **151** 1477–1485

[90] Álvarez-Meza A M, Velásquez-Martínez L F and Castellanos-Dominguez G 2015 *Neurocomputing* **151** 122–129

[91] Tayeb Z, Fedjaev J, Ghaboosi N, Richter C, Everding L, Qu X, Wu Y, Cheng G and Conradt J 2019 *Sensors* **19** 210

[92] Asensio-Cubero J, Gan J Q and Palaniappan R 2016 *Computers in biology and medicine* **68** 21–26

[93] Zhou B, Wu X, Zhang L, Lv Z and Guo X 2014 *Journal of Biosciences and Medicines* **2** 43

[94] Aghaei A S, Mahanta M S and Plataniotis K N 2016 *IEEE Transactions on Biomedical Engineering* **63** 15–29

[95] Lee S B, Kim H J, Kim H, Jeong J H, Lee S W and Kim D J 2019 *Information Sciences*

[96] Dong E, Li C, Li L, Du S, Belkacem A N and Chen C 2017 *Medical & biological engineering & computing* **55** 1809–1818

[97] Aydemir O and Kayikcioglu T 2014 *Journal of neuroscience methods* **229** 68–75

[98] Yi W, Qiu S, Wang K, Qi H, He F, Zhou P, Zhang L and Ming D 2016 *Journal of neuroengineering and rehabilitation* **13** 11

[99] Ge S, Wang R and Yu D 2014 *PloS one* **9** e98019
[100] Nicolas-Alonso L F, Corralejo R, Gomez-Pilar J, Álvarez D and Hornero R 2015 *Neurocomputing* **159** 186–196
[101] Haddad A E and Najafizadeh L 2018 *IEEE Transactions on Biomedical Engineering*
[102] Haddad A and Najafizadeh L 2016 Source-informed segmentation: Towards capturing the dynamics of brain functional networks through EEG *50th Asilomar Conference on Signals, Systems and Computers* pp 1290–1294
[103] Haddad A and Najafizadeh L 2016 Multi-scale analysis of the dynamics of brain functional connectivity using EEG *IEEE Biomedical Circuits and Systems Conference (BioCAS)* pp 240–243
[104] Haddad A, Shamsi F, Ghovanloo M and Najafizadeh L Early decoding of tongue-hand movement from EEG recordings using dynamic functional connectivity graphs *accepted in 9th International IEEE EMBS Conference on Neural Engineering (NER 2019)*
[105] Huo X, Wang J and Ghovanloo M 2008 *Journal of Rehabilitation Research & Development* **45**
[106] Huo X and Ghovanloo* M 2009 *IEEE Transactions on Biomedical Engineering* **56** 1719–1726
[107] Brunner C, Leeb R, Müller-Putz G, Schlögl A and Pfurtscheller G 2008 *Institute for Knowledge Discovery (Laboratory of Brain-Computer Interfaces), Graz University of Technology* **16**
[108] Park H J and Friston K 2013 *Science* **342** 1238411
[109] Haddad A E and Najafizadeh L 2015 Global EEG segmentation using singular value decomposition *2015 37th Annual International Conference of the IEEE Engineering in Medicine and Biology Society (EMBC)* pp 558–561
[110] Haddad A E, Shamsi F and Najafizadeh L 2018 On the spatiotemporal characteristics of class-discriminating functional networks *2018 40th Annual International Conference of the IEEE Engineering in Medicine and Biology Society (EMBC)* pp 1923–1926
[111] Haddad A and Najafizadeh L 2018 Recognizing task-specific dynamic structure of the brain function from EEG *2018 IEEE 15th International Symposium on Biomedical Imaging (ISBI 2018)* pp 712–715
[112] Winter W R, Nunez P L, Ding J and Srinivasan R 2007 *Statistics in Medicine* **26** 3946–3957
[113] Schoffelen J M and Gross J 2009 *Human Brain Mapping* **30** 1857–1865
[114] Carvalhaes C and de Barros J A 2015 *International Journal of Psychophysiology* **97** 174–188
[115] `http://psychophysiology.cpmc.columbia.edu/Software/CSDtoolbox/`
[116] `https://sccn.ucsd.edu/eeglab/`
[117] Rojas G M, Alvarez C, Montoya C E, de la Iglesia-Vayá M, Cisternas J E and Gálvez M 2018 *Frontiers in neuroscience* **12** 235
[118] Moezzi B, Pratti L M, Hordacre B, Graetz L, Berryman C, Lavrencic L M, Ridding M C, Keage H A, McDonnell M D and Goldsworthy M R 2019 *Neuroscience* **422** 230–239
[119] Hata M, Kazui H, Tanaka T, Ishii R, Canuet L, Pascual-Marqui R D, Aoki Y, Ikeda S, Kanemoto H, Yoshiyama K *et al.* 2016 *Clinical Neurophysiology* **127** 1269–1278
[120] Di Lorenzo G, Daverio A, Ferrentino F, Santarnecchi E, Ciabattini F, Monaco L, Lisi G, Barone Y, Di Lorenzo C, Niolu C *et al.* 2015 *Frontiers in human neuroscience* **9** 234
[121] Kim D J, Bolbecker A R, Howell J, Rass O, Sporns O, Hetrick W P, Breier A and O'Donnell B F 2013 *NeuroImage: Clinical* **2** 414–423
[122] Lee S H, Yoon S, Kim J I, Jin S H and Chung C K 2014 *Progress in Neuro-Psychopharmacology and Biological Psychiatry* **51** 51–57
[123] Athanasiou A, Lithari C, Kalogianni K, Klados M A and Bamidis P D 2012 *Advances in Human-Computer Interaction* **2012**
[124] Demuru M, Fara F and Fraschini M 2013 *Journal of integrative neuroscience* **12** 441–447
[125] Shim M, Kim D W, Lee S H and Im C H 2014 *Schizophrenia research* **156** 197–203
[126] Ahmadlou M, Adeli A, Bajo R and Adeli H 2014 *Clinical Neurophysiology* **125** 694–702
[127] Hamedi M, Salleh S H and Noor A M 2016 *Neural computation* **28** 999–1041
[128] Park W, Kwon G H, Kim Y H, Lee J H and Kim L 2016 *Journal of neuroengineering and*

rehabilitation **13** 1–10

[129] López-Larraz E, Ray A M, Figueiredo T C, Bibián C, Birbaumer N and Ramos-Murguialday A 2017 Stroke lesion location influences the decoding of movement intention from eeg *2017 39th Annual International Conference of the IEEE Engineering in Medicine and Biology Society (EMBC)* (IEEE) pp 3065–3068

[130] Ray A M, López-Larraz E, Figueiredo T C, Birbaumer N and Ramos-Murguialday A 2017 Movement-related brain oscillations vary with lesion location in severely paralyzed chronic stroke patients *2017 39th Annual International Conference of the IEEE Engineering in Medicine and Biology Society (EMBC)* (IEEE) pp 1664–1667

[131] Kang J, Wang L, Yan C, Wang J, Liang X and He Y 2011 *Neuroimage* **56** 1222–1234

[132] Hutchison R M, Womelsdorf T, Allen E A, Bandettini P A, Calhoun V D, Corbetta M, Della Penna S, Duyn J H, Glover G H, Gonzalez-Castillo J *et al.* 2013 *Neuroimage* **80** 360–378

[133] Kopell N J, Gritton H J, Whittington M A and Kramer M A 2014 *Neuron* **83** 1319–1328

[134] Bola M and Sabel B A 2015 *Neuroimage* **114** 398–413

[135] Mehrkanoon S, Breakspear M and Boonstra T W 2014 *Brain topography* **27** 338–352

[136] Dimitriadis S I, Laskaris N A, Tsirka V, Vourkas M, Micheloyannis S and Fotopoulos S 2010 *Journal of neuroscience methods* **193** 145–155

[137] Betzel R F, Erickson M A, Abell M, O'Donnell B F, Hetrick W P and Sporns O 2012 *Frontiers in computational neuroscience* **6** 74

[138] Kilner J M, Paulignan Y and Boussaoud D 2004 *Neuroreport* **15** 637–642

[139] Xu L, Zhang H, Hui M, Long Z, Jin Z, Liu Y and Yao L 2014 *Neuroscience* **261** 184–194

[140] Stavrinou M L, Moraru L, Cimponeriu L, Della Penna S and Bezerianos A 2007 *Brain topography* **19** 137–145

[141] Kim Y K, Park E, Lee A, Im C H and Kim Y H 2018 *PLoS One* **13** e0190715

[142] Pitsik E and Frolov N 2020 Network analysis of electrical activity in brain motor cortex during motor execution and motor imagery *Saratov Fall Meeting 2019: Computations and Data Analysis: from Nanoscale Tools to Brain Functions* vol 11459 (International Society for Optics and Photonics) p 1145908

[143] Alimardani F, Boostani R and Blankertz B 2017 *Neural Networks* **92** 69–76

[144] Ang K K, Chin Z Y, Zhang H and Guan C 2008 Filter bank common spatial pattern (fbcsp) in brain-computer interface *2008 IEEE International Joint Conference on Neural Networks (IEEE World Congress on Computational Intelligence)* (IEEE) pp 2390–2397

[145] Thomas K P, Guan C, Tong L C and Prasad V A 2008 An adaptive filter bank for motor imagery based brain computer interface *2008 30th Annual international conference of the IEEE engineering in medicine and biology society* (IEEE) pp 1104–1107

[146] Suk H I and Lee S W 2011 *International Journal of Imaging Systems and Technology* **21** 123–130

Appendix

Table A1: List of Acronyms.

AFNN	Adaptive Fuzzy Neural Network
ANN	Artificial Neural Network
BCI	Brain Computer Interfaces
BPNN	Back-Propagation Neural Network
BTSPRT	Balanced Threshold Sequential Probability Ratio Test
CPMS-CNN	Channel-Projection Mixed-Scale Convolutional Neural Network
CNN	Convolutional Neural Network
CSP	Common Spatial Pattern
DNN	Deep Neural Network
DPL	Dictionary Pair Learning
EEG	Electroencephalography
ELM	Extreme Learning Machine
EOG	Electrooculography
ERD	Event-Related De-synchronization
ERS	Event-Related Synchronization
FIR	Finite Impulse Response
FLDA	Fisher Linear Discriminant Analysis
GA	Genetic Algorithm
GB	Gradient Boosting
GSLDA	Generalized Sparse Linear Discriminant Analysis
HMM	Hidden Markov Model
HS-CNN	Convolutional Neural Network with hybrid Convolution Scale
ICA	Independent Component Analysis
IT2FLS	Interval Type-2 Fuzzy Logic System
kNN	k-Nearest Neighbors
KSVM	Kernel Support Vector Machine
LDA	Linear Discriminant Analysis
LR	Logistic Regression
LRP	Layerwise Relevance Propagation
LS	Least-Square
LSTM	Long Short Term Memory
MDRM	Minimum Distance to Riemannian Mean
ME	Motor Execution
MI	Motor Imagery
MNN	Modified Neural Network
NB	Naive Bayse
NBPW	Naive Bayesian Parzen Window
NN	Neural Network
pCNN	; Spectrogram-based Convolutional Neural Network
PCSP	Probabilistic Common Spatial Pattern
PSO	Particle swarm optimization
RANFN	Recurrent Adaptive Neuro-Fuzzy Network
RBM	Restricted Boltzmann Machines
RCNN	Recurrent Convolutional Neural Network
RF	Random Forest
SBL	Sparse Bayesian Learning
SRC	Sparse Representation-based Classification
SRDA	Spectral Regression Discriminant Analysis
RVM	Relevance Vector Machine
SVD	Singular Value Decomposition
SVM	Support Vector Machine
SUSS-SRKDA	Sequential Updating Semi-Supervised Spectral Regression Kernel Discriminant Analysis
WNB	Weighted Naive Bayesian